ACS APPLIED ELECTRONIC MATERIALS

pubs.acs.org/acsaelm Article

Highly Sensitive and Flexible Capacitive Pressure Sensor Based on a Dual-Structured Nanofiber Membrane as the Dielectric for Attachable Wearable Electronics

Ruiqing Li, Mahyar Panahi-Sarmad, Tianjiao Chen, Ao Wang, Runxin Xu, and Xueliang Xiao*

Cite This: https://doi.org/10.1021/acsaelm.1c01098 Read Online

ACCESS | Metrics & More | Article Recommendations | Supporting Information

ABSTRACT: Wearable devices are an indispensable part of modern life, and flexible capacitive pressure sensors as their luminous subset have assumed a significant role in this day and age owing to ultralow power consumption. In recent years, a fierce debate as well as numerous studies have been conducted to improve the sensitivity of capacitive pressure sensors, but a vital challenge of the mass production of a highly sensitive sensor by a low-cost method still remains. In this paper, to meet industrial demands, we propose a simple method to fabricate sandwich-structured capacitive pressure sensors on an industrial scale and at low cost; as the electrospinning collector, stainless steel screens with regular patterns and structures were utilized to gain the dielectric with both external microstructure and internal pores (dual structure). The prepared pressure sensor is composed of a thermoplastic-urethane electrospun nanofiber film, as a dielectric, in the middle and two conductive woven fabrics on the upper and lower sides as electrodes. Benefiting from the prolific air in the dielectric layer, the designed sensor demonstrates outstanding sensing performance, such as high sensitivity (0.28 kPa^{-1}) in the low-pressure region (0−2 kPa), fast response/relaxation time (65/78 ms), and high-grade durability (1000 cycles). Moreover, the produced pressure sensor is employed for not only detecting human limb movements and object grasping but also detecting pressure distribution in sensor array state, so demonstrating the application potential in attachable wearable electronics.

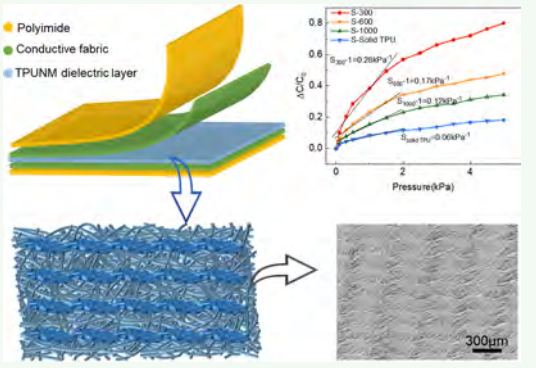

KEYWORDS: *capacitive pressure sensor, electrospinning, nanofiber, sensor array, flexible wearable electronic, dual-structured dielectric layer*

1. INTRODUCTION

Pressure is ubiquitous in daily life, some of them are sensible such as walking, touching, and shaking hands while others are insensible such as physiological signals including pulse, blood pressure, and heartbeat.[1,2] Pressure sensors for detecting pressure and generating monitorable electrical signals from them are prominent. However, traditional pressure sensors that are rigid and heavy need to be updated for practical use in modern applications.[3,4] Therefore, flexible pressure sensors with lightweight and prominent ductility have emerged, enabling excellent application under different shapes, sizes, and conditions.[5] They have drawn considerable attention for promising applications in health monitoring,[6−9] human−machine interaction,[10−12] electronic skin,[13−16] and so forth. Pressure sensors are classified mainly into three different types depending on the output electrical signal, encompassing piezoresistive, capacitive, and piezoelectric.[17−26] Among them, most studies concentrate on piezoresistive and capacitive pressure sensors.[27,28] A piezoresistive pressure sensor possesses the advantages of low cost, simple construction, and low power consumption.[29−31] Meanwhile, it is sensitive to temperature that is able to cause significant errors against abrupt temperature alterations under working conditions.[27] By contrast, a capacitive pressure sensor is independent of change in temperature and has a better stability.[27,32−37] The capacitive pressure sensor, hence, is considered an ideal device for flexible wearable electronics.[33,38−40]

The flexible capacitive pressure sensor enables the conversion of pressure changes into the corresponding capacitance variations. It has the same structure as that of a parallel plate capacitor, with two flexible electrodes and a flexible dielectric layer in the middle.[41] As a consequence of the flexibility of the dielectric layer, even a slight external pressure affects the thickness, leading to a capacitance change of the sensor.[33,42] The properties of the dielectric layer are unquestionably critical for these kinds of sensors. Despite that,

Received: November 6, 2021
Accepted: December 28, 2021

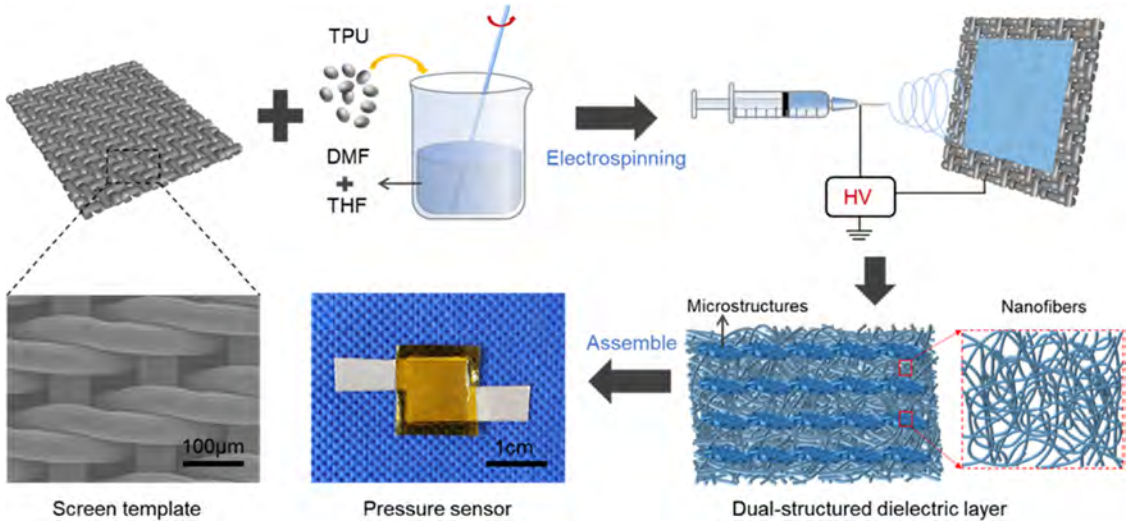

Figure 1. Fabrication of the capacitive pressure sensor with a dual-structured TPUNM dielectric layer.

the common block elastic dielectric materials have a high Young's modulus and low flexibility.[4] These features would cause a small deformation against pressure, thus limiting the sensitivity of the capacitive pressure sensor is expected.[31,34]

Numerous studies have been conducted on improving the sensitivity of the sensor to achieve more remarkable performance, and the pivotal point is to enhance the compressibility of the elastomeric dielectric layer.[43−45] Some studies have modified the surface of the dielectric layer with microstructures to efficiently improve the deformation of the dielectric layer, such as well-known microstructure patterns of pyramidal, conical, and columnar.[46−49] Photolithography or chemical etching is the most common method for preparing well-tuned microstructure templates; however, both of them are expensive and complex.[50] Embedding pores inside the dielectric layer is another approach, allowing a significant increase in the capacitive change that leads to outstanding performance.[36] The construction of porous structures by a sacrificial solvent method is the general idea of most studies using sugar, salt, and foaming agent as sacrificial materials.[5,51−53] This process is genuinely cost-effective and straightforward, but it is still time-consuming and has low chances of large-scale preparation, of course. To sum up, it is desirable to propose a low-cost and simple process with large-scale production potential. Electrospinning, as a shining example, was earlier introduced as a practical and effective technology for preparing flexible porous nanofiber films.[54] Fiber fineness, film thickness, and pore size can be fortunately controlled by changing the parameters during this preparation process.[37] The engineered porous nanofiber membrane showed convenient permeability and compressibility. Therefore, it is capable of great deformation under a wide range of pressure,[49] resulting in it being regarded as an ideal material for the dielectric layer.[30]

In this work, a highly sensitive flexible capacitive pressure sensor based on a dual-structured thermoplastic polyurethane nanofiber membrane (TPUNM) as a dielectric layer was developed by electrospinning technology, composed of a TPUNM dielectric layer and two conductive fabric electrodes. The dual structure (surface microstructure and internal pores) of the dielectric layer was achieved by changing the collector of electrospinning; the stainless steel screen was applied as the collector in this study. The electrospinning process endowed the dielectric layer with a unique porous structure, and the stainless steel mesh collector conferred it with a surface microstructure, thereby enhancing the deformability of the TPUNM dielectric layer. This method has advantages over previous techniques of preparing structured dielectric layers, such as introducing simple, low-cost, and large-scale preparation processes.[55−57] The proposed capacitive pressure sensor represents exceptional sensing performance in terms of high sensitivity (0.28 kPa^{-1}), short response time (65 ms), and good repeatability (1000 cycles), brightening broad application prospects in flexible wearable electronics.

2. EXPERIMENTAL SECTION

2.1. Materials. Thermoplastic polyurethane (TPU) pellets and polyimide (PI) tape were purchased from Shanghai Vita Chemical Reagent Co., Ltd. (Shanghai, China) and Shanghai Mingshen Electronic Technology Development Co., Ltd. (Shanghai, China). *N*,*N*-Dimethylformamide (DMF) and tetrahydrofuran (THF) were bought from Sinopharm Chemical Reagent Co., Ltd. (Shanghai, China). The conductive fabric and stainless steel meshes were obtained from Saintyear Electronic Technologies Co., Ltd. (Zhejiang, China) and a hardware store (Wuxi, China), respectively. Kapton tape was acquired from Rijin Special Electronic Materials Co., Ltd. (Shenzhen, China). All materials were used directly without any further processing and purification.

2.2. Preparation of the Dielectric Layer. The TPU granules were dissolved in DMF and magnetically stirred at 60 °C for 24 h to obtain a uniformly distributed 20 wt % TPU solution. The TPU solution was evenly coated on a glass slide and then the combination (slide + casted solution) was placed in a vacuum drying oven for 10 min to eradicate the bubbles. After that, the solution was dried by processing at 50 °C for 30 min, and the TPU film could be peeled out from the glass slide to obtain the solid TPU dielectric layer.

The TPU particles were dissolved in the organic blending solution, which was the combination of DMF and THF in the mass ratio of 2:3. A 20 wt % TPU electrospinning solution was available after completely dissolving TPU. Also, the stainless steel screen, which was used as a collector, was cleaned with alcohol to ensure the purity of the electrospun membrane. During electrospinning, the ambient temperature was 23 °C, the operating voltage was 10 kV, the distance between the injector and the collector was 10−13 cm, and the feed rate was 0.8 mL/h. Notably, the 300-, 600-, and 1000-mesh stainless steel screens were employed as collectors during the experiment, and the spinning conditions in the three cases were held constant. The TPU solution at the injector head was transformed from a sphere to a

https://doi.org/10.1021/acsaelm.1c01098
ACS Appl. Electron. Mater. XXXX, XXX, XXX−XXX

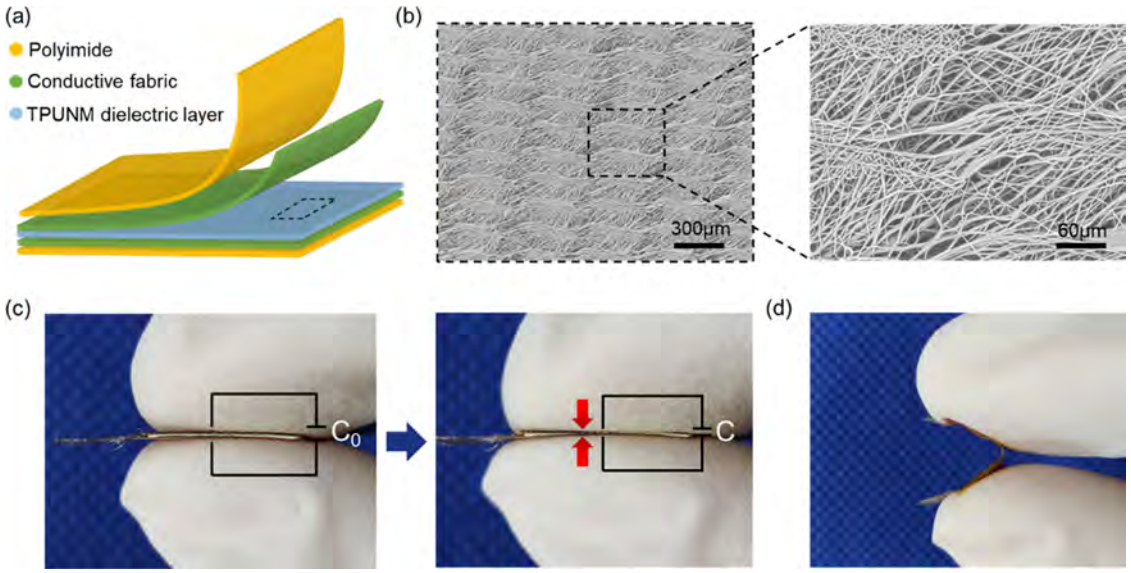

Figure 2. (a) Schematic structure of the capacitive pressure sensor. (b) Scanning electron microscopy (SEM) images of the dual-structured dielectric layer. (c) Working principle diagram of the capacitive pressure sensor. (d) Flexibility of the dual-structured capacitive pressure sensor.

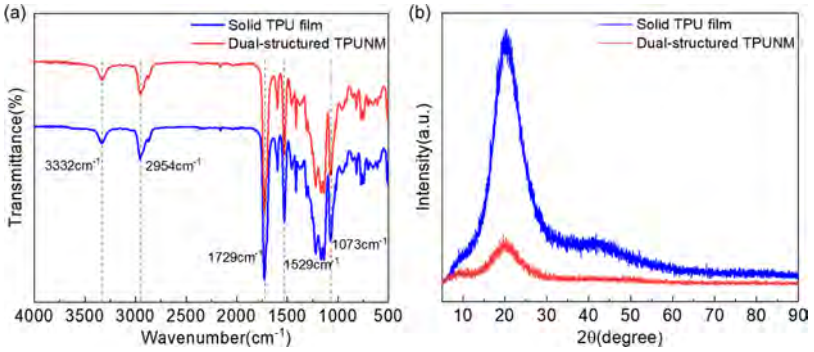

Figure 3. Characterization results of (a) FTIR and (b) XRD spectra of the dual-structured TPUNM and solid TPU film.

cone due to the influence of electrical force and drawn at the tip of the cone to spray onto the stainless steel screen collector with a rough surface. The TPUNM dielectric layer with both unique pores and surface microstructure (dual structure) was obtained after electrospinning and drying, as illustrated in Figure 1.

2.3. Fabrication of the Capacitive Pressure Sensor and Sensor Array. The capacitive pressure sensor consists of two electrodes and a dielectric layer. In this paper, a commercially available woven conductive fabric was utilized as the electrode layer, which could meet the basic structural requirements of the capacitive sensor by stacking it with the TPU dielectric layer in the middle. To ensure the integrity of the sensor, a PI tape was fixed on the outside of the upper and lower electrode layers, also serving as an encapsulation, as shown in Figure 1.

The structure of the sensor array was the same as that of the single sensor in principle. The conductive fabric was cut into eight sample strips with a width of 5 mm. The upper and lower sides of the dielectric layer were placed with four conductive strips, and the upper electrode was perpendicular to the lower electrode. Finally, a 4 × 4 sensor array was assembled by encapsulating the outer side with a PI tape.

2.4. Characterization and Measurements. The structured morphologies of the dielectric layer were detected by scanning electron microscopy (SEM, SU-1510, Hitachi Company, Japan). The chemical structure and the related chemical properties of the dielectric layer were precisely characterized by Fourier transform infrared spectroscopy (FTIR, Nicolet-10, American Thermo Fisher Scientific Co., Ltd., China) in a scan range of 4000−500 cm^{-1}. In addition to studying morphology and chemical structure, an X-ray diffractometer (XRD, D2 PHASER, Brooke AXS Co., Ltd., Germany) was employed to analyze the crystallinity of the dielectric layer in the range of 5−80° at a scanning speed of 0.1°/s.

The foremost components fiercely involved in sensor sensing performance testing are pressure exerting and signal acquisition devices. The dynamic pressure was provided by a universal testing machine (WH-100, Ningbo Weiheng Instrument Co. Ltd., China), and the corresponding capacitance change was acquired by an LCR meter (TH2832, Tonghui Co., Ltd., China) at 1 kHz. As illustrated in Figure S1, the sensor sample was fixed on the sample platform of the universal testing machine and wires were utilized to connect it to the LCR meter. The computer was deployed to set the pressure and record the change in capacitance value.

3. RESULTS AND DISCUSSION

3.1. Structure and Characterization of the Flexible Capacitive Pressure Sensor. The developed flexible capacitive pressure sensor is composed of two conductive fabric layers and an elastomer dual-structured membrane. The compact commercialized woven conductive fabric was utilized as a sensor's electrode, the electrospun TPUNM served as the dielectric layer, and the outermost side was encapsulated with a PI tape to isolate signal interference, as shown in Figure 2a. Figure 2b shows the SEM images of the electrospun TPUNM dielectric layer obtained with a 300-mesh screen template. As mentioned earlier, 300-, 600-, and 1000-mesh screens were

https://doi.org/10.1021/acsaelm.1c01098
ACS Appl. Electron. Mater. XXXX, XXX, XXX−XXX

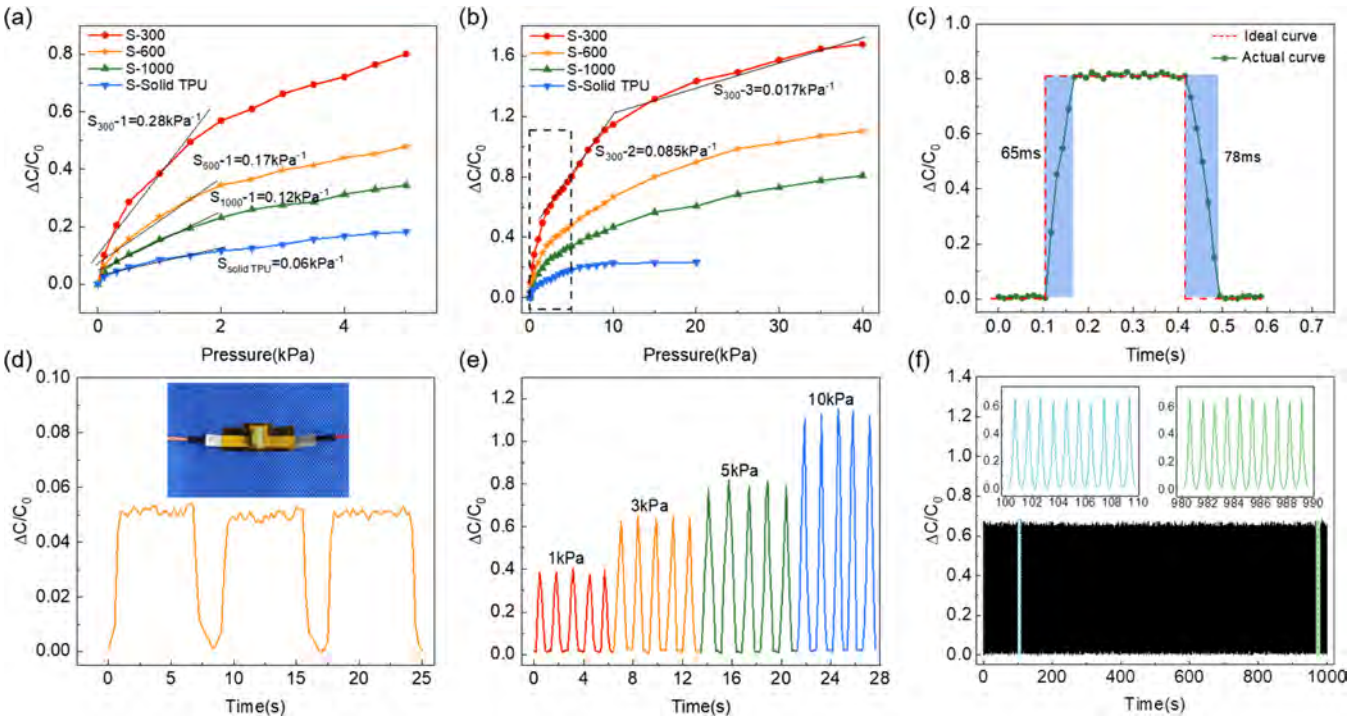

Figure 4. Pressure-sensing performance of the fabricated capacitive pressure sensors: relative capacitance curves of the capacitive pressure sensors with different dielectric layers to a normal pressure of (a) 0−40 kPa and (b) 0−5 kPa. (c) Response and relaxation time of the S-300 pressure sensor under an applied pressure of 5 kPa. (d) Real-time response of the S-300 pressure sensor to small pressure. (e) Capacitance responses of the S-300 pressure sensor under different pressures (1, 3, 5, 10 kPa). (f) Durability and stability of the S-300 pressure sensor response over 1000 cycles under the pressure of 3 kPa.

employed as the electrospinning template in preparing the dielectric layer. As shown in the dielectric layer obtained with a 300-mesh screen, a distinct and uniform microstructure consistent with the screen pattern structure (Figure S2) was achieved at the surface of the dielectric layer; there are many pores inside the film. The other films with 600- and 1000-mesh screens as templates perfectly replicated the structure of the templates, exhibiting analogous microstructures to that of the 300-mesh films (Figure S3). As a result, the sensors composed of these three dielectric layer films are marked as S-300, S-600, and S-1000, respectively. Figure 2c illustrates the working principle of the sensor. The capacitance of the sensor increases under pressure ($C > C_0$), thus enabling the detection of pressure signals. Further, Figure 2d is vividly able to clarify the impressive flexibility of the fabricated sensor.

The FTIR spectra of the electrospun dual-structured TPUNM and the solid TPU film samples are presented in Figure 3a. Regarding the solid TPU film, the absorption peaks at 3332 and 2951 cm^{-1} are attributed to the symmetric stretching vibration of N−H in urethane and the stretching vibration of −C−H, respectively. The stretching vibration peak of C−O−C manifestly appeared at 1073 cm^{-1}. The absorption peaks at 1729 and 1529 cm^{-1} are attributed to the stretching vibration of C═O in urethane and the bending vibration of N−H, which are characteristic absorption peaks of polyester polyurethane. Indeed, these peaks can be found on the spectra of the electrospun dual-structured TPUNM as well, and there are no new absorption peaks, indicating that the electrospinning process, fortunately, failed to disrupt the chemical structure of TPU; it remained intact.

Figure 3b shows the XRD spectra of the electrospun and solid samples. A prominent broad peak at $2\theta = 20°$ is displayed at the solid TPU film sample. This peak is the characteristic peak of polyurethane, which is related to the crystallization characteristics of soft and hard segments.[58] It can be noted that the diffraction peak position of the electrospun dual-structured TPUNM is identical to that of solid TPU film, implying that electrospinning does not change the crystal type of TPU. However, the crystallite size was reduced from 0.92 to 0.78 nm according to the Scherrer formula during the process because of the stretching the chains and inadequate relaxation time.

3.2. Performances of the Pressure Sensor. In this work, the sensing performance was evaluated by applying a normal pressure to the sensor. Sensitivity, which is the most important parameter for analyzing the performance of capacitive pressure sensors, is defined as

$$S = \frac{\Delta C/C_0}{P} \tag{1}$$

where C_0 is the initial capacitance of the sensor, ΔC is the change in capacitance of the sensor ($C - C_0$), and P is the applied pressure. The sensitivity (capacitive response) of S-300, S-600, S-1000, and S-solid TPU is reported in Figure 4a,b; the slope of the curves (ΔC vs P) in the figures represents the sensitivity of sensors. According to the findings, the relative capacitance for all sensors showed an ascending trend with increasing pressure. The sensitivity of the structured (electrospun) sensors is superior to that of the solid TPU sensor (0.06 kPa^{-1}). For instance, in Figure 4a, the sensitivity of solid TPU sensor is half of S-1000, one-thirds of S-600, and one-fifths of S-300 approximately. This solid sensor's drawback is mainly attributed to two reasons. First, the existence of air allows a more considerable deformation of the structured dielectric layer compared to the solid TPU film dielectric layer under the

https://doi.org/10.1021/acsaelm.1c01098
ACS Appl. Electron. Mater. XXXX, XXX, XXX−XXX

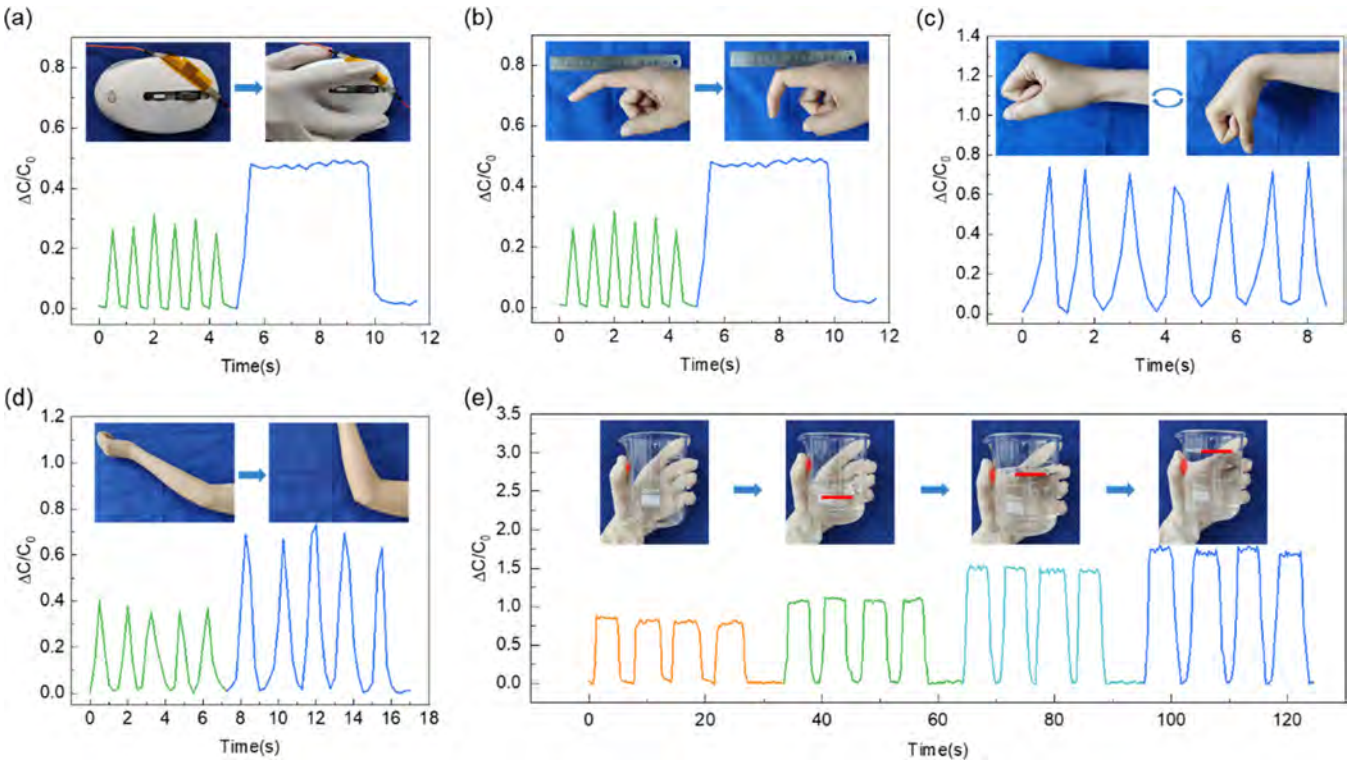

Figure 5. Practical applications of the S-300 pressure sensor: (a) capacitance responses of the sensor when pressing the mouse with the index finger; (b) response curves of the finger joint bending detection; (c) capability of the sensor to detect wrist movements; (d) capacitance responses of the pressure sensor to the elbow movement; and (e) real-time monitoring of the pressure sensor fixed on the thumb when holding beakers of different weights.

same pressure. Second, the dielectric constant (ε_d) was peremptorily changed when the structured dielectric layer is deformed under pressure. Due to the second reason, eqs 2 and 3 are presented as follows

$$\varepsilon_d = V_{air}\varepsilon_{air} + V_{TPU}\varepsilon_{TPU} \quad (2)$$

$$V_{air} + V_{TPU} = 1 \quad (3)$$

where $\varepsilon_{air} = 1$ and ε_{TPU} is about 6.5.[33] The air content of the structured dielectric layer doubtlessly declines under a pressure load, leading to an increase in ε_d. The V_{TPU} of the three dielectric layers was obtained by density ratio of electrospun film to pure TPU film as V_{TPU}-300 = 35.88%, V_{TPU}-600 = 37.36%, and V_{TPU}-1000 = 38.58%. According to the well-known sensor capacitance equation ($C = \varepsilon_0\varepsilon_r A/d$), it is clear that the change in the capacitance of the sensor with a structured dielectric layer is more significant than that of the solid one owing to both the above-mentioned reasons. To further understand the effect of electrospinning on the sensor's performance, the capacitive response of the dual-structured sensor and the microstructured sensor with different pressure loads was studied (Figure S4). The dual-structured sensor adopted the 300-mesh stainless steel screen as the template to prepare the dielectric layer by electrospinning, and the microstructured sensor utilized the same template to develop the dielectric layer through the coating. It is evident from Figure S4 that the sensitivity of the dual-structured sensor is significantly higher than that of the microstructured sensor. This is attributed to a large amount of air introduced by electrospun nanofibers into the dielectric layer, endowing the sensor with a more remarkable capacitance change.

Furthermore, it can be seen from Figure 4b that the maximum sensitivity of the S-300 sensor was 0.28 kPa^{-1}, which is better than that of the S-600 sensor (0.17 kPa^{-1}) and the S-1000 sensor (0.12 kPa^{-1}). It is fiercely dependent on the screen templates. As a rule of thumb, the smaller the mesh count of the screen, the sparser the surface microstructure of the dielectric layer. A sparser microstructure of the dielectric layer resulted in a higher pressure seemingly on the unit structure under the same pressure, thereby making the microstructure easier to compress. In other words, the forces have more chance to focus on smaller−sparser microstructures due to their surface structure. Hence, the S-300 sensor with the minor template mesh count exhibits the highest sensitivity among the three sensors. Above and beyond, it can be observed from the curve that the changes in the capacitance of the S-300 sensor displayed three stages as the pressure increased. In the first stage (<2 kPa), the structured dielectric layer comprises a large amount of air and shows incredible compressibility, and the thickness of the sensor changes by 22.6%. Meanwhile, plenty of air is replaced by the adjacent TPU when persistently compressed, thus improving the dielectric constant of the dielectric layer and endowing the high sensitivity to the sensor (S_{300}-1 = 0.28 kPa^{-1}). As the pressure increases to the second stage (2−10 kPa), the surface and internal structure of the dielectric layer are gradually compressed, leading to greater elastic resistance so that the sensor's sensitivity gradually decreases (S_{300}-2 = 0.085 kPa^{-1}). The thickness of the sensor has changed by 25.3% at this stage. In the third stage (10−40 kPa), the dielectric layer is almost entirely compressed, the thickness of the sensor is only reduced by 9.8%, and the sensor displays a low but stable sensitivity (S_{300}-3 = 0.017 kPa^{-1}). Interestingly, this sensor not

https://doi.org/10.1021/acsaelm.1c01098
ACS Appl. Electron. Mater. XXXX, XXX, XXX−XXX

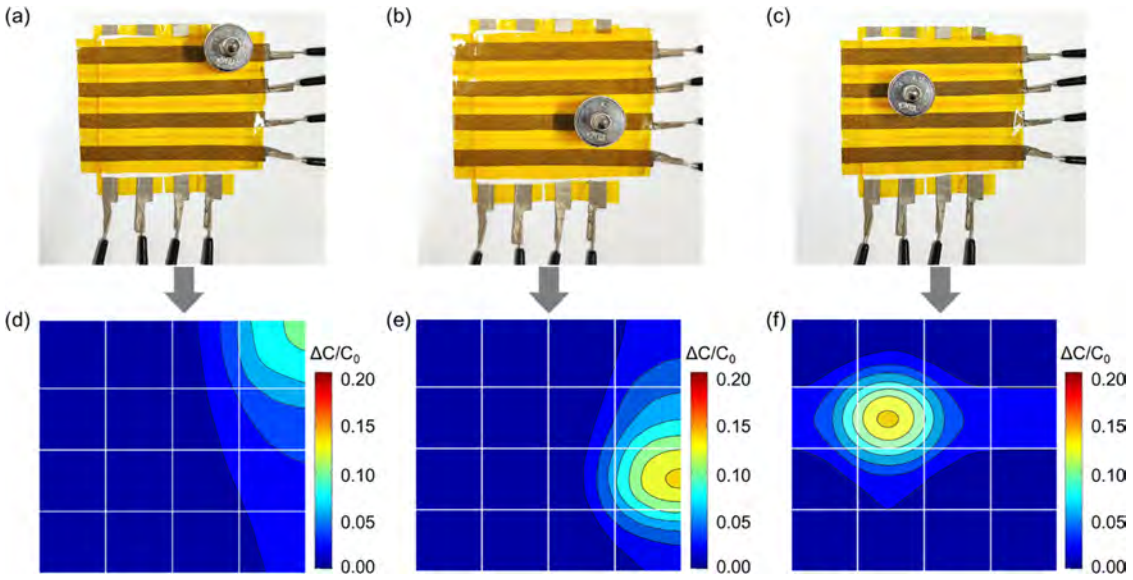

Figure 6. Performance of the 4 × 4 dual-structured sensor array: (a−c) photographs of a 20 g weight are placed at different positions of the sensor array; and (d−f) pressure distribution maps are created by the sensor array's response to the weight.

only has the best sensing performance in the first stage but also outperforms under higher pressure (the other two stages).

After identifying the sensor with the best sensitivity, the dynamic performance of the S-300 sensor was studied, such as response time and repeatability. As shown in Figure 4c, a vertical pressure of about 5 kPa was applied to the sensor to evaluate the response time of the prepared sensor. As a matter of fact, the sensor's relative capacitance increased rapidly from the minimum value to the stable state within 65 ms after loading and dropped to the initial value within 78 ms after the release. Seemingly, the response and relaxation times of the S-300 sensor are less than 100 ms, demonstrating the sensor's fast response capability. Afterward, the sensor's detection of lightweight objects was examined with the aid of a small raisin (≈605 mg). The raisin was placed on the sensor surface, and the alterations of the sensor's relative capacitance were recorded as depicted in Figure 4d, showing that the fabricated sensor was able to respond significantly to a small pressure (60 Pa). As regard to evaluating the responsiveness of the sensor under different pressures, circulating pressures of 1, 3, 5, and 10 kPa were applied to the sensor (see Figure 4e). Based on the observations, the capacitive response of the sensor is principally consistent in five cycles of each pressure, and it grew as the pressure increased, suggesting that the sensor has outstanding pressure resolution ability. As the ultimate test of its performance, 1000 loading/unloading cycles of 3 kPa pressure were conducted to verify the reliability in the prolonged application. The sensor's response is continuous and uniform without notable fatigue, as shown in Figure 4f, which indicates the sensor's strong practicality.

3.3. Applications of the Single Sensor. As assessed earlier, the fabricated sensor has sufficient flexibility and exceptional sensing performance. To verify its potential to meet the needs of human motion detection as a susceptible application, the S-300 sensor was fixed on different human body parts for evaluating its performance in real conditions (Figure 5). The application of the dual-structured sensor in vertical finger pressing is represented in Figure 5a. The sensor was mounted on the left mouse button to record the finger movements (inset of Figure 5a) and the corresponding capacitance change was observed. The relevant curve reveals that the sensor responds immediately and steadily to consecutive clicks and the long-press of the finger; the finger pressure during the long-press stage is greater than that during mouse click. In view of the evidence, the sensor is likely capable of implementing the human joints to detect human movement. As shown in Figure 5b−d, the sensor was attached to the second joint of the index finger, the wrist, and the elbow to detect the capacitive signal, respectively. It is evident that the capacitance of the sensor changes with the movement of human joints, and it can provide a rapid and stable response to repeated movements. Moreover, the capacitance change increased as the same part's motion amplitude increased, indicating that the sensor has the capability to monitor human motion efficiently. Prominently, the sensor could be fixed on the thumb to perceive the grasping of the object, as noted in Figure 5e. The beakers with 0, 100, 200, and 250 mL of water were grasped and put down four times by hand, and the corresponding capacitive response signals were recorded. As observed in Figure 5e, the sensor's capacitance is minimal when grasping an empty beaker. With increasing water volume, the sensor's capacitance signal is intensified gradually, which is chiefly attributed to the increase in beaker weight, requiring the thumb to exert more force to hold the beaker. The sensor's response remains steady during the four grasp-release cycles under each weight. The above demonstrations prove that the proposed dual-structured sensor has excellent application prospects in motion detection, human−computer interaction, and electronic skin.

3.4. Spatial Distinguishing Ability of a 4 × 4 Sensor Array. As a weakness, a single flexible pressure sensor only qualifies for single-point pressure detection. A 4 × 4 capacitive flexible pressure sensor array, therefore, was tailored to confirm the application of the sensor in the detection of pressure spatial distribution. The conductive fabric tapes with a width of 5 mm have been functioning as the electrode material, and the TPUNM with a dual structure has been serving as the porous dielectric layer. The upper and lower electrodes are placed vertically to complete a single sensor (pixel dot) at the intersection of the electrodes, and eventually, there are 16-pixel

https://doi.org/10.1021/acsaelm.1c01098
ACS Appl. Electron. Mater. XXXX, XXX, XXX−XXX

dots in this array. The electrodes are connected to the signal detection module (Figure S5) through wires, and the signal acquisition was carried out by combining the code in MATLAB software. More detail about the pressure distribution detection device is available in the Supporting Information. A small weight (20 g) was placed at different positions of the sensor array (Figure 6a−c) to obtain the corresponding capacitive response map in MATLAB (Figure 6d−f), and Figure S6 shows the corresponding 3D normal capacitive response map in MATLAB. This minor load has been extracted in the detailed figures that the sensor array is accurately able to perceive and monitor the position of the weight, and the capacitance changes that have been generated at the different points are roughly identical. This research paper sets forth a study framework to address the most critical questions to be answered by researchers and industrial men or women who are concerned about the application prospects in object recognition or wearable electronics regarding this type of modern sensor materials.

4. CONCLUSIONS

In summary, the current paper proposed a method to prepare flexible capacitive pressure sensors with an excellent performance by electrospinning, which can meet the needs of low-cost and large-scale preparation. The porous TPUNM dielectric layer with a microstructured surface was successfully fabricated by adopting a stainless steel screen as the electrospinning collector. This primary layer contained the well-meaning amount of air that gave notable feature to significantly deform under slight pressure, thereby providing high sensitivity to the developed sensor. When the 300-mesh screen was employed as the collector, the sensor manifested a high sensitivity of 0.28 kPa^{-1}, a fast response time of 65 ms, remarkable pressure resolution, and reliable durability after 1000 cycles. To prove the practicality, there have been experimental demonstrations in the present research. These results have fiercely asserted that the sensor is able to perceive signals of finger pressing, limb movements, and object grasping. Furthermore, a 4 × 4 multipixel array was prepared with the dual-structured pressure sensor to observe the external pressure distribution. Relying on the sensor's outstanding performance and its simple preparation method, we believe that the proposed sensor has shown potential in a broad range of applications such as health detection, electronic skin, human−computer interaction, and other attachable wearable electronic fields.

■ ASSOCIATED CONTENT

Supporting Information

The Supporting Information is available free of charge at https://pubs.acs.org/doi/10.1021/acsaelm.1c01098.

Experimental setup for testing the sensing performance, SEM image of the 300-mesh, 600-mesh, and 1000-mesh screen templates, SEM images of TPUNM obtained by the 600-mesh and 1000-mesh screen templates, and the photograph of the signal detection module (PDF)

■ AUTHOR INFORMATION

Corresponding Author

Xueliang Xiao − *Key Laboratory of Eco-Textiles, Ministry of Education, Jiangnan University, Wuxi 214122, China;* orcid.org/0000-0003-1898-8267; Email: xiao_xueliang@jiangnan.edu.cn, xiao_xueliang@163.com

Authors

Ruiqing Li − *Key Laboratory of Eco-Textiles, Ministry of Education, Jiangnan University, Wuxi 214122, China;* orcid.org/0000-0001-5001-7116

Mahyar Panahi-Sarmad − *Key Laboratory of Eco-Textiles, Ministry of Education, Jiangnan University, Wuxi 214122, China;* orcid.org/0000-0002-8918-4875

Tianjiao Chen − *Key Laboratory of Eco-Textiles, Ministry of Education, Jiangnan University, Wuxi 214122, China*

Ao Wang − *Key Laboratory of Eco-Textiles, Ministry of Education, Jiangnan University, Wuxi 214122, China*

Runxin Xu − *Key Laboratory of Eco-Textiles, Ministry of Education, Jiangnan University, Wuxi 214122, China*

Complete contact information is available at: https://pubs.acs.org/10.1021/acsaelm.1c01098

Notes

The authors declare no competing financial interest.

■ ACKNOWLEDGMENTS

This work was financially supported by the National Natural Science Foundation of China (Grant No. 51703083) and the Project "Fibre materials and products for emergency support and public safety" from Jiangsu New Horizon Advanced Functional Fibre Innovation Center Co. Ltd. (Grant No. 2020-fx020026).

■ REFERENCES

(1) Zang, Y.; Zhang, F.; Di, C.-a.; Zhu, D. Advances of flexible pressure sensors toward artificial intelligence and health care applications. *Mater. Horiz.* **2015**, *2*, 140−156.

(2) Chen, G.-T.; Su, C.-H.; Wei, S.-H.; Shen, T.-L.; Chung, P.-H.; Guo, Q.-M.; Chen, W.-J.; Chen, Y.-F.; Liao, Y.-C.; Lee, W.-Y. Photocurable ion-enhanced fluorinated elastomers for pressure-sensitive textiles. *Adv. Intell. Syst.* **2020**, *2*, No. 2070041.

(3) Xiong, Y. X.; Hu, Y.; Zhu, P. L.; Sun, R.; Wong, C. P. Fabrication and Application of Flexible Pressure Sensors with Micro/Nano-Structures. *Prog. Chem.* **2019**, *31*, 800−810.

(4) Chen, W.; Yan, X. Progress in achieving high-performance piezoresistive and capacitive flexible pressure sensors: A review. *J. Mater. Sci. Technol.* **2020**, *43*, 175−188.

(5) Chen, S.; Zhuo, B.; Guo, X. Large Area One-Step Facile Processing of Microstructured Elastomeric Dielectric Film for High Sensitivity and Durable Sensing over Wide Pressure Range. *ACS Appl. Mater. Interfaces* **2016**, *8*, 20364−20370.

(6) Chu, Y.; Zhong, J.; Liu, H.; Ma, Y.; Liu, N.; Song, Y.; Liang, J.; Shao, Z.; Sun, Y.; Dong, Y.; Wang, X.; Lin, L. Human Pulse Diagnosis for Medical Assessments Using a Wearable Piezoelectret Sensing System. *Adv. Funct. Mater.* **2018**, *28*, No. 1803413.

(7) Gao, Y.; Ota, H.; Schaler, E. W.; Chen, K.; Zhao, A.; Gao, W.; Fahad, H. M.; Leng, Y.; Zheng, A.; Xiong, F.; Zhang, C.; Tai, L. C.; Zhao, P.; Fearing, R. S.; Javey, A. Wearable Microfluidic Diaphragm Pressure Sensor for Health and Tactile Touch Monitoring. *Adv. Mater.* **2017**, *29*, No. 1701985.

(8) Lou, Z.; Wang, L.; Shen, G. Recent Advances in Smart Wearable Sensing Systems. *Adv. Mater. Technol.* **2018**, *3*, No. 1800444.

(9) Jun, S.; Kim, S. O.; Lee, H.-J.; Han, C. J.; Lee, C.-J.; Yu, Y.-T.; Lee, C.-R.; Ju, B.-K.; Kim, Y.; Kim, J.-W. Transparent, pressure-sensitive, and healable e-skin from a UV-cured polymer comprising dynamic urea bonds. *J. Mater. Chem. A* **2019**, *7*, 3101−3111.

(10) Shi, Q.; Zhang, Z.; Chen, T.; Lee, C. Minimalist and multifunctional human machine interface (HMI) using a flexible wearable triboelectric patch. *Nano Energy* **2019**, *62*, 355−366.

(11) Kim, Y.; Chortos, A.; Xu, W. T.; Liu, Y. X.; Oh, J. Y.; Son, D.; Kang, J.; Foudeh, A. M.; Zhu, C. X.; Lee, Y.; Niu, S. M.; Liu, J.; Pfattner, R.; Bao, Z. N.; Lee, T. W. A bioinspired flexible organic artificial afferent nerve. *Science* **2018**, *360*, 998−1003.
(12) Lee, J.; Kwon, H.; Seo, J.; Shin, S.; Koo, J. H.; Pang, C.; Son, S.; Kim, J. H.; Jang, Y. H.; Kim, D. E.; Lee, T. Conductive fiber-based ultrasensitive textile pressure sensor for wearable electronics. *Adv. Mater.* **2015**, *27*, 2433−2439.
(13) Chen, D.; Pei, Q. Electronic Muscles and Skins: A Review of Soft Sensors and Actuators. *Chem. Rev.* **2017**, *117*, 11239−11268.
(14) Pang, Y.; Zhang, K.; Yang, Z.; Jiang, S.; Ju, Z.; Li, Y.; Wang, X.; Wang, D.; Jian, M.; Zhang, Y.; Liang, R.; Tian, H.; Yang, Y.; Ren, T. L. Epidermis Microstructure Inspired Graphene Pressure Sensor with Random Distributed Spinosum for High Sensitivity and Large Linearity. *ACS Nano* **2018**, *12*, 2346−2354.
(15) Wang, X.; Liu, Z.; Zhang, T. Flexible Sensing Electronics for Wearable/Attachable Health Monitoring. *Small* **2017**, *13*, No. 1602790.
(16) Li, S.; Li, R.; Chen, T.; Xiao, X. Highly Sensitive and Flexible Capacitive Pressure Sensor Enhanced by Weaving of Pyramidal Concavities Staggered in Honeycomb Matrix. *IEEE Sens. J.* **2020**, *20*, 14436−14443.
(17) Masihi, S.; Panahi, M.; Maddipatla, D.; Hanson, A. J.; Bose, A. K.; Hajian, S.; Palaniappan, V.; Narakathu, B. B.; Bazuin, B. J.; Atashbar, M. Z. Highly Sensitive Porous PDMS-Based Capacitive Pressure Sensors Fabricated on Fabric Platform for Wearable Applications. *ACS Sens.* **2021**, *6*, 938−949.
(18) Feng, C.; Yi, Z.; Jin, X.; Seraji, S. M.; Dong, Y.; Kong, L.; Salim, N. Solvent crystallization-induced porous polyurethane/graphene composite foams for pressure sensing. *Composites, Part B* **2020**, *194*, No. 108065.
(19) Lee, J.; Kim, J.; Shin, Y.; Jung, I. Ultra-robust wide-range pressure sensor with fast response based on polyurethane foam doubly coated with conformal silicone rubber and CNT/TPU nanocomposites islands. *Composites, Part B* **2019**, *177*, No. 107364.
(20) Zhang, M.; Wu, Y.; Wang, X.; Wang, X. All-transparent graphene-based flexible pressure sensor array. *Int. J. Mod. Phys. B* **2017**, *31*, No. 1741009.
(21) Wu, Y.; Karakurt, I.; Beker, L.; Kubota, Y.; Xu, R.; Ho, K. Y.; Zhao, S.; Zhong, J.; Zhang, M.; Wang, X.; Lin, L. Piezoresistive stretchable strain sensors with human machine interface demonstrations. *Sens. Actuators, A* **2018**, *279*, 46−52.
(22) Mitrakos, V.; Hands, P. J. W.; Cummins, G.; Macintyre, L.; Denison, F. C.; Flynn, D.; Desmulliez, M. P. Y. Nanocomposite-Based Microstructured Piezoresistive Pressure Sensors for Low-Pressure Measurement Range. *Micromachines* **2018**, *9*, No. 43.
(23) Kim, H. J.; Kim, Y. J. High performance flexible piezoelectric pressure sensor based on CNTs-doped 0−3 ceramic-epoxy nanocomposites. *Mater. Des.* **2018**, *151*, 133−140.
(24) Seo, Y.; Kim, D.; Hall, N. A. Piezoelectric Pressure Sensors for Hypersonic Flow Measurements. *J. Microelectromech. Syst.* **2019**, *28*, 271−278.
(25) Li, S.; Gu, Y.; Wu, G.; Dong, K.; Jia, M.; Zhang, D.; Xiao, X. A flexible piezoresistive sensor with highly elastic weave pattern for motion detection. *Smart Mater. Struct.* **2019**, *28*, No. 035020.
(26) Pang, C.; Lee, G. Y.; Kim, T. I.; Kim, S. M.; Kim, H. N.; Ahn, S. H.; Suh, K. Y. A flexible and highly sensitive strain-gauge sensor using reversible interlocking of nanofibres. *Nat. Mater.* **2012**, *11*, 795−801.
(27) Li, W.; Jin, X.; Zheng, Y.; Chang, X.; Wang, W.; Lin, T.; Zheng, F.; Onyilagha, O.; Zhu, Z. A porous and air gap elastomeric dielectric layer for wearable capacitive pressure sensor with high sensitivity and a wide detection range. *J. Mater. Chem. C* **2020**, *8*, 11468−11476.
(28) Tseng, Y.-T.; Lin, Y.-C.; Shih, C.-C.; Hsieh, H.-C.; Lee, W.-Y.; Chiu, Y.-C.; Chen, W.-C. Morphology and properties of PEDOT:PSS/soft polymer blends through hydrogen bonding interaction and their pressure sensor application. *J. Mater. Chem. C* **2020**, *8*, 6013−6024.
(29) Li, W.-D.; Pu, J.-H.; Zhao, X.; Jia, J.; Ke, K.; Bao, R.-Y.; Liu, Z.-Y.; Yang, M.-B.; Yang, W. Scalable fabrication of flexible piezoresistive pressure sensors based on occluded microstructures for subtle pressure and force waveform detection. *J. Mater. Chem. C* **2020**, *8*, 16774−16783.
(30) Yang, X.; Wang, Y.; Qing, X. A flexible capacitive sensor based on the electrospun PVDF nanofiber membrane with carbon nanotubes. *Sens. Actuators, A* **2019**, *299*, No. 111579.
(31) Xu, F.; Li, X.; Shi, Y.; Li, L.; Wang, W.; He, L.; Liu, R. Recent Developments for Flexible Pressure Sensors: A Review. *Micromachines* **2018**, *9*, No. 580.
(32) Wang, J.; Suzuki, R.; Shao, M.; Gillot, F.; Shiratori, S. Capacitive Pressure Sensor with Wide-Range, Bendable, and High Sensitivity Based on the Bionic Komochi Konbu Structure and Cu/Ni Nanofiber Network. *ACS Appl. Mater. Interfaces* **2019**, *11*, 11928−11935.
(33) Atalay, O.; Atalay, A.; Gafford, J.; Walsh, C. A Highly Sensitive Capacitive-Based Soft Pressure Sensor Based on a Conductive Fabric and a Microporous Dielectric Layer. *Adv. Mater. Technol.* **2017**, *3*, No. 1700237.
(34) Zeng, X.; Wang, Z.; Zhang, H.; Yang, W.; Xiang, L.; Zhao, Z.; Peng, L. M.; Hu, Y. Tunable, Ultrasensitive, and Flexible Pressure Sensors Based on Wrinkled Microstructures for Electronic Skins. *ACS Appl. Mater. Interfaces* **2019**, *11*, 21218−21226.
(35) Vu, C. C.; Kim, J. Highly elastic capacitive pressure sensor based on smart textiles for full-range human motion monitoring. *Sens. Actuators, A* **2020**, *314*, No. 112029.
(36) Wang, X.; Xia, Z.; Zhao, C.; Huang, P.; Zhao, S.; Gao, M.; Nie, J. Microstructured flexible capacitive sensor with high sensitivity based on carbon fiber-filled conductive silicon rubber. *Sens. Actuators, A* **2020**, *312*, No. 112147.
(37) Jin, T.; Pan, Y.; Jeon, G. J.; Yeom, H. I.; Zhang, S.; Paik, K. W.; Park, S. K. Ultrathin Nanofibrous Membranes Containing Insulating Microbeads for Highly Sensitive Flexible Pressure Sensors. *ACS Appl. Mater. Interfaces* **2020**, *12*, 13348−13359.
(38) Li, M.; Liang, J.; Wang, X.; Zhang, M. Ultra-Sensitive Flexible Pressure Sensor Based on Microstructured Electrode. *Sensors* **2020**, *20*, No. 371.
(39) Wan, S.; Bi, H.; Zhou, Y.; Xie, X.; Su, S.; Yin, K.; Sun, L. Graphene oxide as high-performance dielectric materials for capacitive pressure sensors. *Carbon* **2017**, *114*, 209−216.
(40) Li, R.; Zhou, Q.; Bi, Y.; Cao, S.; Xia, X.; Yang, A.; Li, S.; Xiao, X. Research progress of flexible capacitive pressure sensor for sensitivity enhancement approaches. *Sens. Actuators, A* **2021**, *321*, No. 112425.
(41) Park, S. W.; Das, P. S.; Chhetry, A.; Park, J. Y. A Flexible Capacitive Pressure Sensor for Wearable Respiration Monitoring System. *IEEE Sens. J.* **2017**, *17*, 6558−6564.
(42) Yao, S.; Zhu, Y. Wearable multifunctional sensors using printed stretchable conductors made of silver nanowires. *Nanoscale* **2014**, *6*, 2345−2352.
(43) Luo, Y.; Shao, J.; Chen, S.; Chen, X.; Tian, H.; Li, X.; Wang, L.; Wang, D.; Lu, B. Flexible Capacitive Pressure Sensor Enhanced by Tilted Micropillar Arrays. *ACS Appl. Mater. Interfaces* **2019**, *11*, 17796−17803.
(44) Boutry, C. M.; Nguyen, A.; Lawal, Q. O.; Chortos, A.; Rondeau-Gagne, S.; Bao, Z. A Sensitive and Biodegradable Pressure Sensor Array for Cardiovascular Monitoring. *Adv. Mater.* **2015**, *27*, 6954−6961.
(45) Shao, J.; Chen, X.; Li, X.; Tian, H.; Wang, C.; Lu, B. Nanoimprint lithography for the manufacturing of flexible electronics. *Sci. China Technol. Sci.* **2019**, *62*, 175−198.
(46) Pignanelli, J.; Schlingman, K.; Carmichael, T. B.; Rondeau-Gagné, S.; Ahamed, M. J. A comparative analysis of capacitive-based flexible PDMS pressure sensors. *Sens. Actuators, A* **2019**, *285*, 427−436.
(47) Xiong, Y.; Shen, Y.; Tian, L.; Hu, Y.; Zhu, P.; Sun, R.; Wong, C.-P. A flexible, ultra-highly sensitive and stable capacitive pressure sensor with convex microarrays for motion and health monitoring. *Nano Energy* **2020**, *70*, No. 104436.

https://doi.org/10.1021/acsaelm.1c01098
ACS Appl. Electron. Mater. XXXX, XXX, XXX−XXX

(48) Asghar, W.; Li, F.; Zhou, Y.; Wu, Y.; Yu, Z.; Li, S.; Tang, D.; Han, X.; Shang, J.; Liu, Y.; Li, R. W. Piezocapacitive Flexible E-Skin Pressure Sensors Having Magnetically Grown Microstructures. *Adv. Mater. Technol.* **2020**, *5*, No. 1900934.
(49) Kim, S. J.; Yang, H.; Oh, J. H.; et al. Simple fabrication of highly sensitive capacitive pressure sensors using a porous dielectric layer with cone-shaped patterns. *Mater. Des.* **2021**, *14*, No. 197.
(50) Mahata, C.; Algadi, H.; Lee, J.; Kim, S.; Lee, T. Biomimetic-inspired micro-nano hierarchical structures for capacitive pressure sensor applications. *Measurement* **2020**, *151*, No. 107095.
(51) Hwang, J.; Kim, Y.; Yang, H.; Oh, J. H. Fabrication of hierarchically porous structured PDMS composites and their application as a flexible capacitive pressure sensor. *Composites, Part B* **2021**, *211*, No. 108607.
(52) Park, S. W.; Das, P. S.; Park, J. Y. Development of wearable and flexible insole type capacitive pressure sensor for continuous gait signal analysis. *Org. Electron.* **2018**, *53*, 213−220.
(53) Chhetry, A.; Yoon, H.; Park, J. Y. A flexible and highly sensitive capacitive pressure sensor based on conductive fibers with a microporous dielectric for wearable electronics. *J. Mater. Chem. C* **2017**, *5*, 10068−10076.
(54) Lin, M.-F.; Xiong, J.; Wang, J.; Parida, K.; Lee, P. S. Core-shell nanofiber mats for tactile pressure sensor and nanogenerator applications. *Nano Energy* **2018**, *44*, 248−255.
(55) Niu, H.; Gao, S.; Yue, W.; Li, Y.; Zhou, W.; Liu, H. Highly Morphology-Controllable and Highly Sensitive Capacitive Tactile Sensor Based on Epidermis-Dermis-Inspired Interlocked Asymmetric-Nanocone Arrays for Detection of Tiny Pressure. *Small* **2020**, *16*, No. 1904774.
(56) Guo, Y.; Gao, S.; Yue, W.; Zhang, C.; Li, Y. Anodized Aluminum Oxide-Assisted Low-Cost Flexible Capacitive Pressure Sensors Based on Double-Sided Nanopillars by a Facile Fabrication Method. *ACS Appl. Mater. Interfaces* **2019**, *11*, 48594−48603.
(57) Park, J.; Lee, Y.; Hong, J.; Lee, Y.; Ha, M.; Jung, Y.; Lim, H.; Kim, S. Y.; Ko, H. Tactile-Direction-Sensitive and Stretchable Electronic Skins Based on Human-Skin-Inspired Interlocked Microstructures. *ACS Nano* **2014**, *8*, 12020−12029.
(58) Li, S.; Li, R.; González, O. G.; Chen, T.; Xiao, X. Highly sensitive and flexible piezoresistive sensor based on c-MWCNTs decorated TPU electrospun fibrous network for human motion detection. *Compos. Sci. Technol.* **2021**, *203*, No. 108617.

https://doi.org/10.1021/acsaelm.1c01098
ACS Appl. Electron. Mater. XXXX, XXX, XXX−XXX